Industrial Engineering Journal
ISSN: 0970-2555
Volume : 53, Issue 9, September : 2024

ANALYSIS OF SINGLE POINT INCREMENTAL PROCESS TO FABRICATE ALUMIUMIUM ALLOY HEMISPERICAL CUPS

E.Akhil*, G. Devendar, A. Chennakesava Reddy

*PG student, Department of Mechanical Engineering, JNTUH Collage of Engineering, India
Assistant Professor, Department of Mechanical Engineering, JNTUH Collage of Engineering, India
Senior Professor, Department of Mechanical Engineering, JNTUH Collage of Engineering, India.

ABSTRACT

This project focuses on the Single Point Incremental Forming (SPIF) process to fabricate hemispherical cups using AA 5053. The method involves gradually shaping a fixed sheet into the desired form through incremental deformation, employing a hemispherical or ball-nose tool controlled numerically in a single point incremental sheet forming process. Finite element analysis was conducted using the ABAQUS 6.14 package. To evaluate the influence of process parameters such as step depth, tool radius, sheet thickness, and coefficient of friction on the stresses and strains induced in the sheet, and to identify key process parameters, experiments were designed employing the Taguchi technique and ANOVA method.
KEYWORDS: incremental forming process, AA5053, tool radius, sheet thickness, coefficient of friction, hemispherical cups.

INTRODUCTION

Incremental sheet forming is a method that gradually deforms a sheet using a round-tipped tool, causing localized plastic deformation along a predetermined path until the final part is achieved. This innovative approach addresses numerous challenges in the manufacturing industry, including concerns related to quality, complexity, and production cost, leading to its increasing adoption over conventional sheet forming methods.

Initially, sheet metal operations primarily involved techniques such as pressing, spinning, and deep drawing. Spinning involves rapidly rotating a metal disc to shape it into an axially symmetric item, while deep drawing mechanically pulls a sheet of metal radially into a forming die.

Recent research in the deep drawing process has focused on warm deep drawing to enhance the super plastic properties of various materials, including AA2219[2], AA2618[3], AA3003[4], AA5049[5], 1050A [6], AA1050-H18 [7], 1070AA[12] alloy, EDD steel, and gas cylinder steel. Researchers have also explored the fabrication of different cup shapes, such as pyramidal, rectangular, and cone cups. The formability of these cups depends on several factors.

OBJECTIVE OF WORK

The objective of this work is to enhance the attractiveness of Single Point Incremental Forming (SPIF) as a manufacturing process within the industry. This is achieved by deepening our fundamental understanding of the process and its formability.

In this study, the focus was on comprehending the formability aspect of SPIF, specifically in the context of single point incremental deep drawing of hemispherical cups made from AA5053 sheet material. To accomplish this, a well planned experimental design was conducted, utilizing the Taguchi Technique. The actual single point incremental deep drawing process was executed with the assistance of finite element analysis software called ABAQUS.

Industrial Engineering Journal
ISSN: 0970-2555
Volume : 53, Issue 9, September : 2024

MATERIALS AND METHODS

ABAQUS was selected for simulating the single point incremental sheet forming process due to its efficient dynamic analysis capabilities and ability to yield reliable results, distinguishing it from other software options. Additionally, a brief overview of the study on hemispherical cups and the utilization of the Taguchi Technique for optimizing process parameters is presented at the conclusion of this chapter. Detailed information on the process parameters and their respective levels is provided.

Chemical Composition of AA5053: This table likely lists the specific elements and their respective proportions that make up the alloy. It's common to find elements like aluminum (Al), magnesium (Mg), and perhaps small amounts of other alloying elements like manganese (Mn) or chromium (Cr).

Table 1: Chemical composition of AA5053

Element	Silicon	Chromium	Copper	Magnesium	Manganese	Zinc	Iron	Aluminum
% weight	<0.25	0.15-0.35	<0.10	2.2-2.8	<0.10	<0.10	<0.40	Balance

Mechanical Properties of AA5053: This table likely summarizes key mechanical properties of the alloy. Typical properties include tensile strength, yield strength, elongation, hardness, and others that are important for understanding how the material performs under different conditions.

Table 2: Mechanical Properties of AA5053

Material	Density (Kg/m^3)	Young Modulus (Gpa)	Yield Strength (Mpa)	Ultimate Strength (Mpa)	Elongation at fracture %	Flow stress (Mpa)
AA5053	2680	67	100	250	15	$\sigma = 414 * \epsilon^{0.27}$

Plasticity: The data of the material in the plastic zone needed for the modeling of incremental sheet metal forming process was taken from the True Stress - True Strain curve in the figure1.

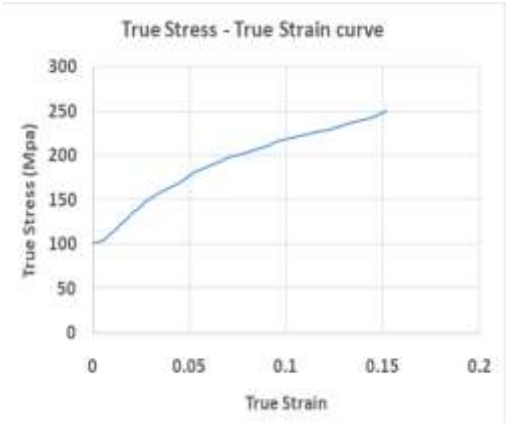

Figure 1: True Stress – True Strain curve

DESIGN OF EXPERIMENTS

In the present work on Single Point Incremental Forming (SPIF), chosen four controllable process parameters, each with three levels. This experimental design has been summarized in Table.

To efficiently conduct experiments and finite element analysis (FEA) using ABAQUS software opted for an orthogonal array (OA), specifically L9. OA matrices are used for design of experiments to systematically vary factors and assess their impact on the outcomes.

Table 3: Process Parameters and levels

Factor	Symbol	Level 1	Level 2	Level 3
Sheet thickness(mm)	A	0.8	1	1.2
Step depth(mm)	B	0.5	0.75	1
Tool radius(mm)	C	4	6	8
Coefficient of friction	D	0.05	0.1	0.15

Industrial Engineering Journal
ISSN: 0970-2555
Volume : 53, Issue 9, September : 2024

Table 4: Orthogonal array (L9) and control parameters

Trail No.	A	B	C	D
1	3	1	3	2
2	1	1	2	2
3	1	3	1	3
4	2	2	2	3
5	2	1	3	3
6	2	3	1	1
7	1	2	3	1
8	3	3	1	2
9	3	2	2	1

Finite Element Modeling

The Finite Element Method (FEM) has become a crucial tool for solving various engineering problems.

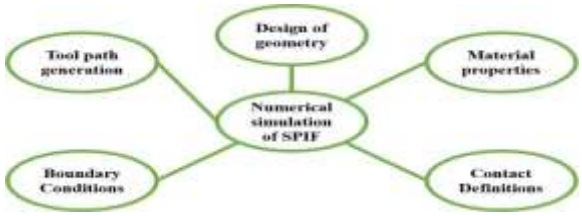

Figure 2: Schematic representation of Pre-processing steps in ABAQUS

Geometric Modeling: In geometric modeling a square sheet of dimensions 150 mm x 150, and tool of cylindrical rod with hemispherical end with different radii 4 mm, 6 mm and mm, 8 mm were created. The two parts, sheet and tool were created as 3D deformable shell planar and analytically rigid body respectively, and assembled together as shown in figure 3.

Figure 3: Assembly of sheet and tool.

Mesh generation: Meshing is a process the process of discretizing the component. Here the sheet is meshed as shown in the figure with quad dominated S4R shell element.

Mesh size: 2 mm
Number of nodes: 5776
Number of elements: 5625

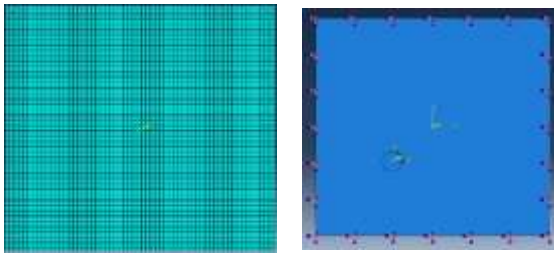

Figure 4: Sheet with generated Mesh and Boundary Conditions

Tool Path Definition: In the present work, the tool path profile as shown in the figure was used to generate hemispherical shape.

TOOL PATH PROFILE

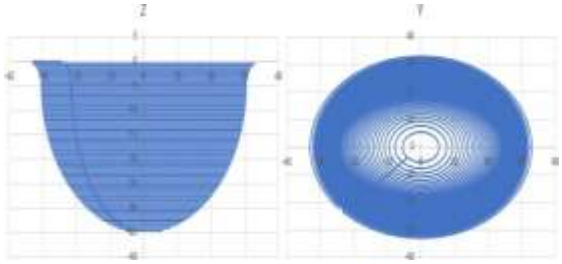

Figure 5: Tool path profile

POST-PROCESSING

After completion of finite element analysis of single point incremental deep drawing process of hemispherical cups, results were extracted from the output database file which was generated by ABAQUS during simulation of SPIP. For all trials, induced von Mises stress, stress components (S11, S12, S22), maximum principle strain, minimum principle strain, equivalent plastic strain, stress triaxiliaty and strain rate were extracted along the path. Output

Industrial Engineering Journal
ISSN: 0970-2555
Volume : 53, Issue 9, September : 2024

data of sheet thickness of every trial was extracted along the path as shown in figure 6.

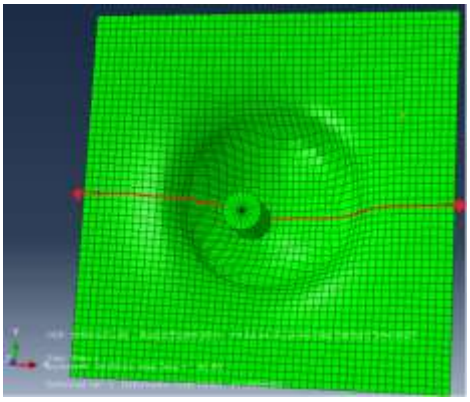

Figure 6: Deformed shape of sheet

RESULTS AND DISCUSSION

It was supposed that the rotating cylindrical tool had a rigid body. Additionally, three linear motions were applied to the cylindrical tool in the x, y, and z directions to outline the cup's contour. Along its borders, the sheet was given fixed displacement boundary constraints.

Influence of process parameters on effective stress

Von Mises stress decreases as the tool radius and coefficient of friction increase. This suggests that larger tool radii and reduced friction contribute to lower stress levels during SPIF. These findings can help form the basis for optimizing the forming process to achieve desired results by illuminating how various parameters impact stress distribution during SPIF.

For the trials 1, 2, 3, 4, 5, 6, 7, 8 and 9, the von Mises stresses are, respectively, 536, 402.9, 476, 470, 496, 454, 423, 539, and 436 MPa as shown in Figure 7.

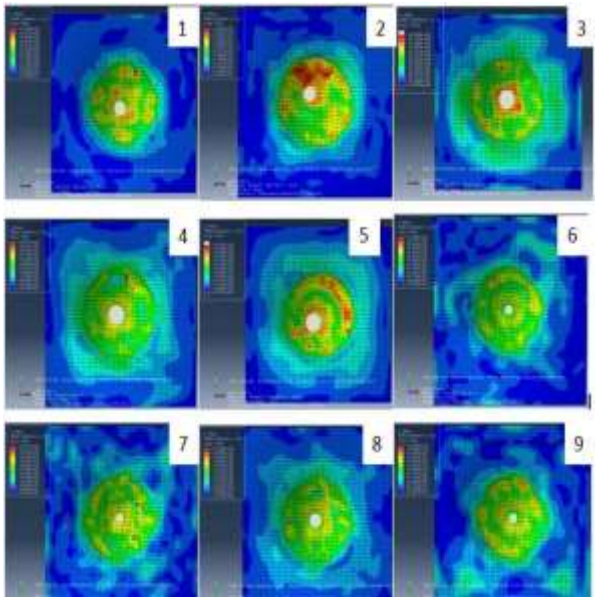

Figure 7: Raster images of Von Mises stress in the hemispherical cups.

Table 5: Analysis of Variance for Means

Source	DF	Seq SS	Adj SS	Adj MS	F	P	contribution
Sheet thickness	2	86.2	86.2	43.11	*	*	0.47
Step depth	2	1008.2	1008.2	504.11	*	*	5.57
Tool radius	2	8262.9	8262.9	4131.44	*	*	45.71
Coefficient of friction	2	8716.2	8716.2	4358.11	*	*	48.22
Total	8	18073.6					100

From the table 5 we can find that almost two parameters tool radius and coefficient of friction contributes in equal percentages.

Table 6: Response Table for Means

Level	Sheet thickness	Step depth	Tool radius	Coefficient of friction
1	471.3	476.3	509.7	489.3
2	473.3	479.0	436.0	426.3
3	466.0	455.3	465.0	495.0
Delta	7.3	23.7	73.7	68.7
Rank	4	3	1	2

Industrial Engineering Journal
ISSN: 0970-2555
Volume : 53, Issue 9, September : 2024

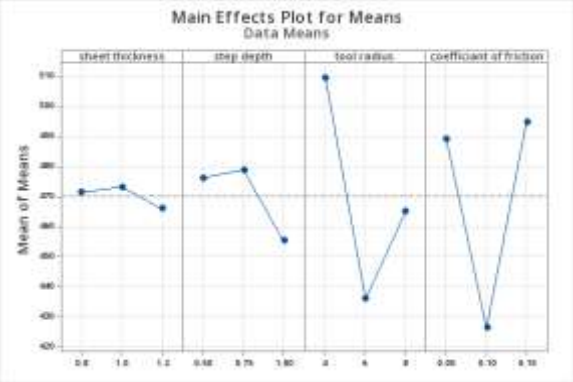

Figure 8: Effect of process parameters on stress

Influence of parameters on strain rate

The relationship between sheet thickness and strain rate is intriguingly detailed in Figure 8. Notably, as the sheet thickness increases within the range of 0.8 to 1.2 mm, the strain rate experiences a gradual decrease. However, it's worth highlighting a peculiar trend once the sheet thickness reaches 1.2 mm, there's a slight upturn in the strain rate.

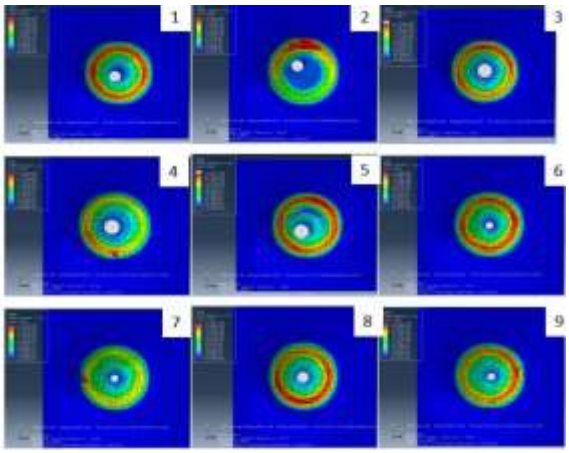

Figure 9: Raster images of Equivalent plastic strain (PEEQ) in the hemispherical cups.

Figure 9 draws attention to another key observation that the strain rate tends to be notably higher when utilizing a tool radius of 5 mm during the plastic deformation of the sheet material. This underscores the influence of tool geometry on the forming process.

Furthermore, it's imperative to recognize the pivotal role of friction in this process. According to Coulomb's law of friction ($\tau = \mu Fn$ where Fn represents the normal pressure), the frictional shear stress is directly proportional to the coefficient of friction (COF).

Table 7: Analysis of Variance for Means

Source	DF	Seq SS	Adj SS	Adj MS	F	P	contribution
Sheet thickness	2	6.3582	6.3582	3.17908	*	*	35.55
Step depth	2	1.4388	1.4388	0.71941	*	*	8.03
Tool radius	2	6.7307	6.7307	3.36534	*	*	37.60
Coefficient of friction	2	3.3690	3.3690	1.68448	*	*	18.82
Total	8	17.8966					100

Table 8: Response Table for Means

Level	Sheet thickness	Step depth	Tool radius	Coefficient of friction
1	17.86	19.04	18.96	18.66
2	18.97	18.38	19.95	18.33
3	19.92	19.33	17.83	19.76
Delta	2.06	0.96	2.12	1.43
Rank	2	4	1	3

From table 8 we can find that tool radius is one of important factor in strain rates as it ranks first and from graph we can consider that as tool radius at 5mm maximum strain rate occurs and then decreases.

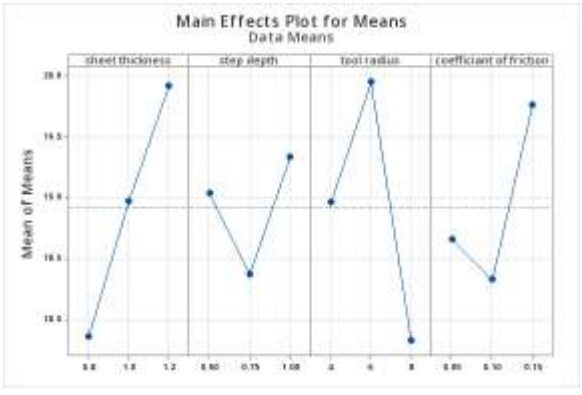

Figure 10: Effect of process parameters on strain

Industrial Engineering Journal
ISSN: 0970-2555
Volume : 53, Issue 9, September : 2024

Influence of parameters on thickness reduction

The relationship between sheet thickness and the reduction in sheet thickness is clearly evident, as depicted in Figure 11.

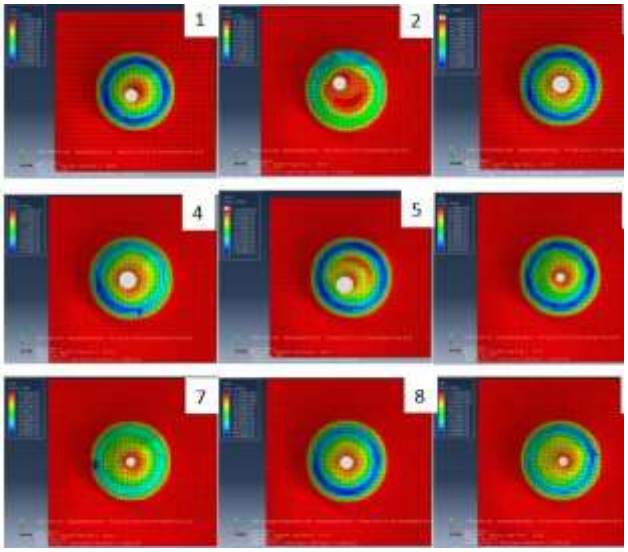

Figure 11: Raster images of Thickness of sheet in the hemispherical cups for trials 1 to 9.

This observation reveals that as the sheet thickness increases, the reduction in thickness becomes more pronounced.

Table 9: Analysis of Variance for Means

Source	DF	Seq SS	Adj SS	Adj MS	F	P	contribution
Sheet thickness	2	0.026667	0.026667	0.013333	*	*	11.1
Step depth	2	0.000000	0.000000	0.000000	*	*	0
Tool radius	2	0.1066667	0.106667	0.0533333	*	*	44.41
Coefficient of friction	2	0.1066667	0.106667	0.0533333	*	*	44.41
Total	8	0.24000					100

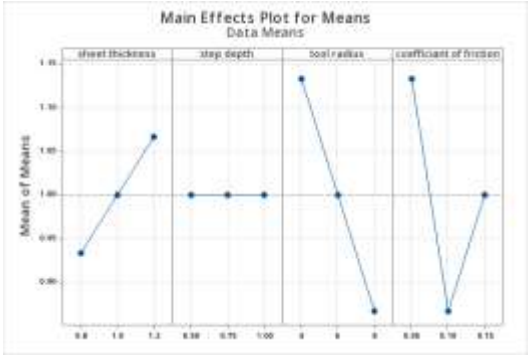

Figure 12: Effect of process parameters on sheet thickness

To assess the thickness reduction, the analysis focuses on the centerline of the deformed cup, as illustrated in Figure 13. Notably, the examination of this figure 10 unveils an interesting pattern the majority of the thickness reduction occurs in the cup's walls, with less significant changes observed in the flange or the bottom of the cup.

Table 10: Response Table for Means

Level	Sheet thickness	Step depth	Tool radius	Coefficient of friction
1	0.9333	1.0000	1.133	1.1333
2	1.0000	1.0000	1.000	0.8667
3	1.0667	1.0000	0.866	1.0000
Delta	0.1333	0.0000	0.266	0.2667
Rank	3	4	1.5	1.5

Interestingly, here tool radius and coefficient of friction contributes in equal half to the stress values in 1.5 and 1.5 ranks as shown in response table 10.

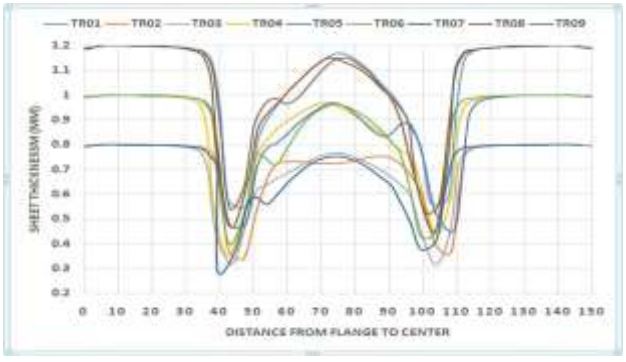

Figure 13: Location of thickness reduction in deformed cup.

CONCLUSIONS

Notably, the sheet thickness, tool radius and coefficient of friction are the most important variables in this study since it significantly affects the formability limit diagram of AA5053. The three most important ones are step size, sheet thickness, and coefficient of friction. Together, these elements influence how the forming process behaves and produces its results.

From the analysis we can find that for the aluminum alloy of AA5053 provided L9 orthogonal trails the most influencing parameters are tool radius and coefficient of friction which contributes equally.

REFERENCES

1. A. Chennakesava Reddy, Finite element analysis of reverse superplastic blow forming ofTi-Al-4V alloy for optimized control of thickness variation using ABAQUS, Journal ofManufacturing Engineering, National Engineering College, vol. 1, no. 1, pp. 6-9, 2006.

2. A. C. Reddy, Formability of High Temperature and High Strain Rate Super-plastic Deep Drawing Process for AA2219 Cylindrical Cups, International Journal of Advanced Research, vol. 3, no. 10, pp. 1016-1024, 2015.

3. C. R Alavala, High temperature and high strain rate superplastic deep draw-ing process for AA2618 alloy cylindrical cups, International Journal of Scientif-ic Engineering and Applied Science, vol. 2, no. 2, pp. 35-41, 2016.

4. C. R Alavala, Practicability of High Temperature and High Strain Rate Super-plastic Deep Drawing Process for AA3003 Alloy Cylindrical Cups, Interna-tional Journal of Engineering Inventions, vol. 5, no. 3, pp. 16-23, 2016.

5. C. R Alavala, High temperature and high strain rate superplastic deep draw-ing process for AA5049 alloy cylindrical cups, International Journal of Engi-neering Sciences & Research Technology, vol. 5, no. 2, pp. 261-268, 2016.

6. A. C. Reddy, Homogenization and Parametric Consequence of Warm Deep Drawing Process for 1050A Aluminum Alloy: Validation through FEA, International Journal of Science and Research, vol. 4, no. 4, pp. 2034-2042, 2015.

7. A. C. Reddy, Formability of Warm Deep Drawing Process for AA1050-H18 Pyramidal Cups, International Journal of Science and Research, vol. 4, no. 7, pp. 2111-2119, 2015.

8. Lambiase, F., & Di Ilio, A. (2018). Joining Aluminum with Titanium alloy sheets by mechanical clinching. Journal of Manufacturing Processes, 35, 457-465.

9. A. C. Reddy, Formability of super plastic deep drawing process with moving blank holder for AA1050-H18 conical cups, International Journal of Research in Engineering and Technology, vol. 4, no. 8, pp. 124-132, 2015.

10. A. C. Reddy, Performance of Warm Deep Drawing Process for AA1050 Cylindrical Cupswith and Without Blank Holding Force, International Journal of Scientific Research, vol.4, no. 10, pp. 358-365, 2015.

11. A. C. Reddy, Necessity of Strain Hardening to Augment Load Bearing Capacity ofAA1050/AlN Nano composites, International Journal of Advanced Research, vol. 3, no. 6,pp. 1211-1219, 2015.

12.Kothapalli Chandini, A. C. Reddy, Parametric Importance of Warm Deep Drawing Processfor 1070A Aluminium Alloy: Validation through FEA, International Journal of Scientific& Engineering Research, vol. 6, no. 4, pp. 399-407, 2015.